Wang, Z., **Shen, Q.**, Hua, P., Jiang, S., Li, R., Li, Y., Fan, G., Zhang, J., Krebs, P. (2020):
Characterizing the anthropogenic-induced trace elements in an urban aquatic environment: A source apportionment and risk assessment with uncertainty consideration
J. Environ. Manage. **275** , art. 111288

Characterizing the anthropogenic-induced trace elements in an urban aquatic environment: a source apportionment and risk assessment with uncertainty consideration

Zhenyu Wang[a, b, 1], Qiushi Shen[c, d, e, f, 1], Pei Hua[a, *], Shanshan Jiang[f], Ruifei Li[b], Yunben Li[c, g], Gongduan Fan[g], Jin Zhang[h], and Peter Krebs[b]

[a] SCNU Environmental Research Institute, Guangdong Provincial Key Laboratory of Chemical Pollution and Environmental Safety & MOE Key Laboratory of Environmental Theoretical Chemistry, South China Normal University, 510006 Guangzhou, China

[b] Institute of Urban and Industrial Water Management, Technische Universität Dresden, 01062 Dresden, Germany

[c] State Key Laboratory of Lake Science and Environment, Nanjing Institute of Geography and Limnology, Chinese Academy of Sciences, Nanjing 210008, China

[d] Department of Lake Research, UFZ - Helmholtz Centre for Environmental Research, Magdeburg 39114, Germany.

[e] Sino-Africa Joint Research Center, Chinese Academy of Sciences, Wuhan 430074, China

[f] East Africa Great Lakes and Urban Ecosystem Joint Research Station, Nanjing Institute of Geography and Limnology, Chinese Academy of Sciences, Dar es Salaam P.O. Box 9750, Tanzania

[g] College of Civil Engineering, Fuzhou University, 350108 Fuzhou, China

[h] Institute of Groundwater and Earth Sciences, Jinan University, 510632 Guangzhou, China

1 These authors contributed equally to this work

*Corresponding author:

jzhang@jnu.edu.cn (J. Zhang);

pei.hua@hotmail.com (P. Hua)

Keywords

Trace elements; Self-organizing map; Positive matrix factorization; Stochastic risk assessment; Uncertainty analysis

Abstract

The spatial distribution of water quality status, especially in water bodies near intensively urbanized areas, is tightly associated with patterns of human activities. For establishing a robust assessment of the sediment quality in an urban aquatic environment, the source apportionment and risk assessment of Cr, Mn, Ni, Cu, Zn, As, Cd, Hg, and Pb in sediments from an anthropogenic-influenced lake were carried out with considering uncertainties from the analysis methods, random errors in the sample population and the spatial sediment heterogeneity. The distribution analysis of the trace metals with inverse distance weighting-determined method showed that the pollutants were concentrated in the middle and southern areas of the lake. According to the self-organizing map and constrained positive matrix factorization receptor model, agricultural sources (24.8%), industrial and vehicular sources (42.5%), and geogenic natural sources (32.7%) were the primary contributors to the given metals. The geogenic natural had the largest random errors, but the overall result was reliable according to the uncertainty analysis. Furthermore, the stochastic contamination and ecological risk models identified a moderate/considerable contamination level and a moderate ecological risk to the urban aquatic ecosystem. With consideration of uncertainties from the spatial heterogeneity, the contamination level of Hg, and the ecological risk of Cd in had a 20-30% probability of the increase.

1. INTRODUCTION

Water resources are vital for human survival and sustainable development of urban regions (Chen et al., 2019; Kaeseberg et al., 2018; Li et al., 2019b; Wang et al., 2019c). However, the unprecedented increase in population and rapid growth of urbanization has relevant impacts on the quality of the urban aquatic environment (Ayeni et al., 2011; Chen et al., 2019; Chetelat and Gaillardet, 2005; Zhang et al., 2017b). On one hand, several anthropogenic activities, including agrochemical usage (Li et al., 2014; Marrugo-Negrete et al., 2017; Zhang et al., 2017a), industrial practices (Cheung et al., 2003; Jain, 2004; Quevauviller et al., 1989; Zhang et al., 2015a), and traffic (Men et al., 2019; Pekey et al., 2004; Sutherland, 2000; Zhang et al., 2019b) are potential drivers of the deterioration of the quality of water resources. On the other hand, the land surface modification in highly-urbanized areas alters the regional hydrological processes of infiltration and runoff. The increasing amount of surface runoff with non-point source pollutants flows into the water bodies near the urban area, causing the water quality degradation in the urban aquatic environment (Chen et al., 2017; Luo et al., 2020; Qin et al., 2010; Tong and Chen, 2002). In consequence, water pollution in the urban aquatic environment is a major concern. As a typical urban aquatic environment, the urban water channel has been regarded as the fore-end part of the natural water bodies and the primary pollutant carrier that receives wastewater and polluted surface runoff. The variation of anthropogenic associated pollutants makes it difficult for cities to maintain a good status of urban surface waters.

Among these pollutants, trace metals have drawn a wide concern as they have toxicity, persistence, bioaccumulation, and biomagnification (Lin et al., 2013; Raghunath et al., 1999; Yang et al., 2014). In the aquatic environment, sediment is recognized as the main sink for trace metals, thereby posing long-term serious risks to benthic organisms and, in turn, humans (Fu et al., 2013; Ning et al., 2014; Yi et al., 2011). Therefore, the trace metal pollution in sediments can be a typical indicator revealing the impact of anthropogenic activities on the aquatic environment. As the first step to improve the quality status of urban water channels, it is essential to evaluate the spatial variation of trace metals, identify major source contributors to trace metals, and understand their contamination characterization in the sediments.

Cluster analysis is an adopted method to evaluate the spatial variation in water quality in the water resources and ecosystems (Li et al., 2019a; Nguyen et al., 2020). More recently, self-organizing map (SOM) was frequently used as a clustering method to spatially analyze water quality due to its good noise tolerant and ability to handle complex data with non-linear relationships, missing data and outliers (Alvarez-Guerra et al., 2008; Guo et al., 2020; Li et al., 2018a). The visualization map with clustering information yielded by SOM can enhance the understanding of trace metal pollution in the urban water channels.

Conventional source apportionment approaches (e.g., principal component analysis; PCA) and pollution assessment approaches (e.g., contamination factor and ecological risk factor models) are commonly used to identify the source contributors

(Lin et al., 2016; Shil and Singh, 2019; Wijesiri et al., 2019) and assess trace metal pollution risk in sediments, respectively (Cao et al., 2018; Hossain et al., 2019; Liang et al., 2016). However, such approaches have limits in interpreting the uncertainty of the samples caused by sampling errors, measurement errors, and sediment heterogeneity (Feng et al., 2019b; Norris et al., 2014), and it is hard to judge the fitness of the result as a basis for decision making.

The analysis of uncertainty can overcome these problems and improve the reliability of the results. Regarding the source apportionment, it could improve the solution especially if small datasets were used (Manousakas et al., 2017), and could be a useful method to judge the accurate number of sources (Brown et al., 2015b). Besides, the uncertainty consideration could also increase the robustness of the solution in risk assessments (Park et al., 2019). Several mathematical approaches with uncertainty consideration, such as the positive matrix factorization (PMF) receptor model for source apportionment (Niu et al., 2019; Wang et al., 2019c) and the advanced stochastic model considering probability theory for pollution assessment (Feng et al., 2019a) have been newly developed, but not been applied for pollution assessment in the urban aquatic environment.

Accordingly, the primary focus of this study was to conduct the source apportionment and risk assessment with uncertainty consideration to facilitate the source-oriented mitigation of trace metals in the urban aquatic environment. The detailed objectives were to: (1) characterize the spatial distribution of the trace elemental contents in urban aquatic sediments, (2) identify the major contributor(s) of the trace metals through an artificial neural network of self-organizing map model and constrained PMF receptor model associated with uncertainty analysis, and (3) assess the pollution and ecological risk levels based on a stochastic contamination model and ecological risk determination model with uncertainty consideration.

2. MATERIALS AND METHODS

2.1 Study area

The study area was Wanshan Lake (31° 35' 34.78" N, 120° 31' 4.17" E), which is the largest lake on the west bank of the Wangyu River in the Taihu catchment, China. It is situated east of Xishan District in Wuxi (396.8 km^2) and adjacent to Suzhou. It has a planimetric area of 1.9 km^2 with an average depth of 1.12 m (0.65 - 4.2 m) (JPDWR, 2006). The annual precipitation and mean temperature are 1,048 mm and 18°C, respectively, in the study area. It is a typical urban aquatic environment that connects the downtown area of Wuxi, the Wangyu River, and Taihu Lake. Therefore, the pollutant status in Wanshan Lake could be regarded as an indicator of the regional aquatic environment.

Nine trace metals (Cr, Mn, Ni, Cu, Zn, As, Cd, Hg, and Pb) in sediments was monitored at 30 sampling sites, namely, 10 sites (N1–N10), 7 sites (M1–M7), and 13 sites (S1–S13) in the northern, middle, and southern area of the channel, respectively as given in **Fig. 1a**.

2.2 Sampling and chemical analysis

The sampling and field surveys were conducted in April 2019. Three parallel sediment samples were collected at depths of 0–3 cm at each sampling site using a bucket dredger, transferred into polyethylene ziploc bags, and stored in a freezer at -20 °C in the laboratory. To analyze the trace metals (Cr, Mn, Ni, Cu, Zn, As, Cd, Hg, and Pb) in the sediments, the samples were freeze-dried (Biosafer-10A lyophiliser) and subsequently sieved with a 200-mesh nylon sieve after being carefully ground.

After microwave-assisted digestion, the determination of trace elements was conducted by a TAS-986AFG atomic absorption spectrophotometer, 240ZAA graphite furnace atomic absorption spectrometer, or PF32 atomic fluorescence spectrometer according to GB/T 22105.2-2008 (As), GB/T 17141-1997 (Cd and Pb), HJ 491-2009 (Cr), GB/T 17138-1997 (Cu and Zn), GB/T 17139-1997 (Ni), and LY/T 1256-1999/5.2 (Mn) standards. The limit of detection for each metal was 5.000 mg/kg for Cd, 5.000 mg/kg for Mn, 5.000 mg/kg for Ni, 1.000 mg/kg for Cu, 5.000 mg/kg for Zn, 1.000 mg/kg for As, 0.010 mg/kg for Cd, 0.002 mg/kg for Hg, and 0.100 mg/kg for Pb.

2.3 Geostatistical analysis

Inverse distance weighting (IDW) has simple computation and straightforward interpretable features, thus it is used extensively for analyzing the spatial distribution of pollutants in sediments (Dai et al., 2018; Gu and Gao, 2019; Li et al., 2013). IDW method with a weighting power of 2.0 was conducted to illuminate the spatial variation of the trace metal concentrations and source contributions (Fang et al., 2019b; Gu and

Gao, 2019). The geostatistical analysis was implemented by QGIS 3.2 with the coordinate reference system of WGS 84. The GIS information of Wanshan Lake was provided by Nanjing Institute of Geography and Limnology, Chinese Academy of Sciences.

2.4 Self-organising map (SOM)

The dimensionality reduction is conducted in a way that neurons or units in the SOM, which are represented by the weight vector, are trained to find the minimum distance to the input vector by the best matching unit (Alvarez-Guerra et al., 2008; Kiang, 2001). Euclidean metrics were used to calculate the distance between the vectors in this study. The detailed algorithms were provided by Kohonen (1990). The unit setting was described in **Supplementary Material Part B**.

The SOM clustering was yielded by the K-means algorithm, and the optimal clustering was found according to the lowest Davies–Bouldin validity index (DBI) (Davies and Bouldin, 1979). All SOM calculations in the study were performed using SOM toolbox 2.1 in the MATLAB R2017b platform (Vesanto et al., 2000).

2.5 Positive matrix factorisation (PMF)

The identification and apportionment of pollutant sources were conducted by PMF receptor model 5.0 released by the United States Environmental Protection Agency. Non-negativity constraints were imposed in the PMF, and the missing data points and outliers were down-weighted employing a point-by-point estimation of uncertainty (Jain et al., 2018; Zhang et al., 2019a).

The uncertainties of the PMF results including the random errors and rotational ambiguity were analyzed by the Bootstrap (BS) method and Displacement (DISP) method. BS method can identify the disproportionately influence of the observations on the PMF solution, or random errors, which describe a variation in the sample population (Paatero et al., 2014). The DISP method is able to explicitly determine the rotational ambiguity of a PMF solution which is an uncertainty generated by the PMF receptor model (Brown et al., 2015a). The uncertainties could be visualized as the upper uncertainty interval, an increase of uncertainty estimates from the base factor concentration to the BS or DISP upper uncertainty limits.

The result with the lowest PMF object function in 200 realizations was selected in the study, and a constraint method was applied to reduce the effect of rotational ambiguity. The PMF algorithm, pre-treatment of input data, determination of the PMF parameters and constrained model operation were described in detail in **Supplementary Material Part A**. The detailed computation of PMF was described by Comero et al. (2009) and Norris et al. (2014). The source identification referred to the review of source fingerprints of each element for individual potential sources summarised in **Table S1**.

2.6 Stochastic contamination and ecological risk determination model

The conventional contamination factor (CF) model and ecological risk factor (ER) model are widely used to evaluate the contamination level and ecological risk condition of trace metals in sediments according to the following equations:

CF (Cabrera et al., 1999; Tomlinson et al., 1980):

$$CF_i = \frac{C_i}{C_{ref,i}} \qquad \text{Eq. 1}$$

where C_i and $C_{ref,i}$ are the content value and background level of the i^{th} specific element observed in sediments, respectively.

ER (Hakanson, 1980):

$$ER_i = Tr_i \times CF_i \qquad \text{Eq. 2}$$

where the value of *Tr* is 40 for Hg, 30 for Cd, 10 for As, 5 for Pb, Ni, and Cu, 2 for Cr, and 1 for Mn and Zn (Hakanson, 1980; Sharifi et al., 2016).

The *CF* index can rank the sediment quality according to four classes of contamination levels, namely, low ($CF < 1$), moderate ($1 \leq CF < 3$), considerable ($3 \leq CF < 6$), and very high ($CF \geq 6$), while the *ER* can describe five classes of potential ecological risk levels, namely, low ($ER < 40$), moderate ($40 \leq ER < 80$), considerable ($80 \leq ER < 160$), high ($160 \leq ER < 320$), and very high ($ER \geq 320$).

However, C_i in the model cannot describe the uncertainty of spatial sediment heterogeneity (Sharifi et al., 2016), which can be overcome by the stochastic contamination model (SCM) and ecological risk determination model (SERM), which are developed based on probability theory. C_i is not a concrete value but lies in the interval $[a_i, b_i]$. In this study, a_i and b_i were defined as the first quartile (Q1) and third quartile (Q3), respectively, of the concentration values of the i^{th} trace element in the northern, middle, or southern area of the channel to avoid biased results caused by extreme values. The maximum entropy principle determined the uniform statistical distribution of C_i within the interval, and the possibility of the contamination and the ecological risk condition of the pollutants in each corresponding class was calculated based on the interval and the classification standards of CF and ER. The detailed computation is elaborated in **Supplementary Material Part C**.

3. RESULTS AND DISCUSSION

3.1 Spatial distribution of trace metals in sediments

Descriptive information of Cr, Mn, Ni, Cu, Zn, As, Cd, Hg, and Pb in the sediments of the study area as well as the geogenic background value in sediments are listed in **Table 1**. The background values of trace elements were referenced from their content contained in Xiashu loess owing to the strong effect of loess on the river sediments in the Taihu Basin (Bian et al., 2016). The average elemental contents in the sediments followed a descending order of concentrations as follows: Mn (696.90 mg/kg) > Zn (418.07 mg/kg) > Cr (152.90 mg/kg) > Cu (103.86 mg/kg) > Ni (88.69 mg/kg) > Pb (17.38 mg/kg) > As (14.00 mg/kg) > Hg (0.17 mg/kg) > Cd (0.10 mg/kg). All trace metal concentrations, except for Mn and Pb, exceeded the corresponding background levels. Comparable to the published data in the other rivers/lakes in China (**Table 1**), the contents of Cr, Ni, Cu, and Zn in the sediments of the study area were significantly higher than those found in other studies, ranging from 65.79 mg/kg (Qin et al., 2015) to 151.00 mg/kg (Jiang et al., 2018) for Cr; 23.60 mg/kg (Yan et al., 2016) to 43.00 mg/kg (Bian et al., 2016) for Ni; 21.80 mg/kg (Wang et al., 2019b) to 86.00 mg/kg

(Bian et al., 2016) for Cu; 68.4 mg/kg (Yan et al., 2016) to 224.00 mg/kg (Jiang et al., 2018) for Zn. The aforementioned results indicate a strong influence of anthropogenic activities on trace element pollution in the studied urban channel.

The coefficient of variation of Cu (78.12%), Cd (62.58%), and Cr (60.10%) showed the large spatial heterogeneity of these metal concentrations. Its values of the other trace metals were in the range of 28.67–44.65%. The spatial distribution of the content in sediments (**Fig. 1b-e**) shows that the pollutants tended to be concentrated in the middle or southern area of the channel. The concentrations in the middle area and the southern area were 18%-91% and 6%-92% higher on average than those in the northern area. Most of the elements, except for Mn, showed the maximum content in sediments at M6 which should be affected by a particular source.

3.2 Cluster analysis according to the self-organizing map

According to the SOM component distribution as shown in **Fig. 2a**, the trace metals were classified into three interpretable groups. Group I was characterized by Cr, Ni, Cu, Zn, Cd, and Hg owing to their significant similarity with high values (red) in the sites at the bottom-right corner and relatively low values (blue) in the top-left corner. These elements mostly originate from anthropogenic sources, such as industrial activities, traffic, and agricultural work (Adekola and Eletta, 2007; Li et al., 2018b; Omwene et al., 2018; Zhang et al., 2018). Group II and III, characterized by As and Mn respectively, displayed completely different component distributions. The component distribution of Pb illustrated both outlook patterns of II and III, which means that Pb content in sediments was possibly influenced simultaneously by the contributors found in these two groups.

Fig. 2b showed clusters of the sampling sites and four different clusters (clusters I–IV) were classified by the K-means algorithm. The distance between the map units and the diagram of the DBI against the number of clusters is shown in **Fig. S1** and **S2**. Cluster I was characterized as an As-influenced area. It grouped the sites (N6, N8, M1, S12, and S13) with a considerably high content of only As in sediments in the range of 17.0–21.5 mg/kg. Cluster II was the low-concentration area, which included seven northern sites, two middle sites, and three southern sites. Comparatively, Cluster III contained 10 sites that are all located at the middle or southern parts of the channel with relatively higher concentrations of trace elements monitored. The last three sites (I9, L1, and M3) were distinguished as Cluster IV. They shared a common feature in that they had considerably higher concentrations of varied pollutants than those of the other sites. The maximum concentrations of Zn (761.00 mg/kg) and Hg (0.34 mg/kg) were found at N10, while most of the pollutants showed significantly high content in sediments at M5 and especially M6.

3.3 Spatial changes in the sources of trace elements

3.3.1 Source identification

The fractional contributions of three factors to the elements are illustrated in **Fig. 3a**. Factor 1 was characterized by Cd, Cu, and Hg with the contributions of 68.35%, 45.73%, and 54.76%. Cd and Hg are traditionally found in many agrochemical applications, such as fungicides, pesticides, and phosphate fertilizers (Dai et al., 2018; Ji et al., 2019; Wang et al., 2018; Yang et al., 2009). Cu is also related to seed disinfectants and herbicides for agricultural purposes (Ruiz-Fernández et al., 2009). It is a widely used element in Chinese approved agrochemicals, and 5000 tons of Cu is estimated to be used in farmland in China (Chen et al., 2016). Hence Factor 1 might be associated with the agricultural sources.

Factor 2 explained high loadings of Cu (42.85%), Zn (43.42%), Cr (42.25%), and Ni (34.36%). Cu and Zn are extensively found in auto brake erosion, road and pavement erosion, vehicle wear, and other traffic-related activities (Adekola and Eletta, 2007; Pekey et al., 2004; Sutherland, 2000; Zhang et al., 2015b). Cu, Zn, Cr, and Ni can be released into the environment through metal plating, metal casting, fuel combustion, leather production, and other industrial activities (Özmen et al., 2004; Wang et al., 2018; Wang et al., 2019c; Yang et al., 2009; Zhang and Qu, 2001). It also explained 42.10% of Mn, which possibly caused by industrial sources including goods processing and welding (Pinsino et al., 2012). Therefore, Factor 2 probably represented industrial and vehicular sources.

Factor 3 explained the significant loadings of As (57.43%), Pb (55.62%), and Mn (43.86%). Mn bound with As could have originated from the weathering of parent minerals and paedogenic processes (Yin et al., 2011; Zaharescu et al., 2009). Pb was the only element that had below-background concentrations in the study. Thus, Factor 3 might be interpreted as geogenic natural sources.

3.3.2 Influence of local economic structure on contributor distribution

Agricultural sources, industrial and vehicular sources, and geogenic natural sources accounted for 24.8%, 42.5%, and 32.8% of the total metals respectively according to the PMF results. The source contributions in mg/kg in the entire Wanshan Lake were spatially distributed in **Fig. 3b-d**. The results almost matched the patterns of land use types near the channel (**Fig. S4**). The contribution of agriculture mainly existed in the middle area and part of the northern area where a large area of agricultural land and green land was located. N10 was a representative site near farming land where the highest contribution of 938.5 mg/kg occurred. Conversely, there was a significant occurrence of industry and vehicle in the southern area (averagely 923.7 mg/kg), which was surrounded by several industrial areas and manufacturing plants.

Furthermore, according to the Chinese Statistical Yearbook that the industrial wastewater emissions from the downtown area of Wuxi were 35.17 tons per capita in 2017, which was considerably higher than that in Jiangsu Province (averagely 22.42 tons per capita), Beijing (3.92 tons per capita), and Shanghai (13.07 tons per capita). Additionally, the gross domestic product of primary and secondary industries in Wuxi accounted for 3.3% and 12.8% (2^{nd} place), respectively, in 2017 in Jiangsu Province. This reveals that agriculture and industry are the two dominant factors in the economic structure in the intensively urbanized city of Wuxi, which was consistent with the source apportionment from this study.

3.3.3 Uncertainty analysis

The uncertainty intervals between the constrained-based factor concentration of all trace metals and the upper uncertainty limits for BS method and DISP method were illustrated in **Fig. 4**. The ratio between the upper uncertainty intervals and the PMF-simulated concentrations, expressed as the uncertainty ratio, was 19% (Ni) to 96% (Cd) for BS method and 28% (As) to 45% (Mn) for DISP for all metals in total concentration. The BS upper uncertainty intervals of Cu, As, Cd, Hg, and Pb in all three sources were higher than those for DISP method. Here, the upper uncertainty intervals for BS method of Cd in agricultural sources (0.04 mg/kg) were nearly 4 times higher than those for DISP method (0.01 mg/kg). The BS intervals of Mn in agricultural sources as well as industrial and vehicular sources (78.38 mg/kg; 150.12 mg/kg) were approximated to DISP intervals (80.62 mg/kg; 189.85 mg/kg). The results indicate that the random error of the most metals was more dominant than rotational ambiguity (Wu et al., 2019). It can be explained by the fact that the effect of rotational ambiguity was reduced by the constraint method but the small datasets resulted in the increase of random errors.

Among three sources, the uncertainty ratios for BS/DISP were in the range of 4%-100%/13%-103% for agricultural, 2%-187%/8%-114% for industrial and vehicular, and 51%-270%/16%-181% for geogenic natural sources. Obviously, the factors of agricultural sources as well as industrial and vehicular sources demonstrated fewer uncertainties than geogenic natural sources, indicating a robust identification of these two source contributors. The large uncertainty ratio of geogenic natural sources resulted in high uncertainty in this factor, suggesting a poorly-defined factor. As, for characterizing the factor, was the metal with the worst fitting score (r^2 = 0.5001) determined by PMF receptor model (**Fig. S3**). The result of SOM also demonstrated two independent clusters characterized by As and Mn. Both reasons suggest that information characterized by As in PMF could cause the increase of uncertainty of geogenic natural sources and overestimate the contribution of the factor.

Nevertheless, all PMF results were still reliable according to the > 95% BS mapping factors and the zero swap for dQmax for DISP method (**Supplementary Material Part 1**).

3.4 Contamination and ecological risk assessment

The contamination level and ecological risk of each trace element in the northern, middle, and southern parts of the channel were identified by the SCM and SERM, and the results are illustrated in **Fig. 5** and **Table S2**. The uncertainty of the spatial sediment heterogeneity was described as the probability distribution in the classes of contamination level and ecological risk. Additionally, Mn was not considered in the risk assessment owing to the lack of background information and its low toxicity in a non-acidic environment.

Fig. 5a shows that Pb showed low contamination levels in the water channel while Cr, Ni, As, Cd, and Pb reached moderate contamination levels. The contamination levels (probability in %) of Cu, Hg, and Zn in the northern area were moderate (93%), moderate (100%), and considerable (100%), respectively, while those in the middle/southern area were considerable (100%/80%), considerable (100%/0%), and very high (70%/76%), respectively. Considering the spatial variation of contamination, the highest metal contamination was found in the middle area, whereas the lowest was found in the northern area. Hg in the north and south had 18% and 4% probability, respectively, in moderate contamination levels but could possibly deteriorate the water quality to the next contamination category.

As shown in **Fig. 5b**, Most elements were identified as posing low risks to the aquatic ecosystem. However, Hg showed a significantly higher ecological risk. Besides, the presence of Cd in the northern and southern areas had probabilities of 30% and 21%, respectively, increasing the ecological risk from low to moderate.

The relatively lower contamination level and ecological risk in the northern area were caused by the fact that the northern area of the channel was developed as a pilot wetland where the water quality was significantly improved. In contrast, the channels in the middle and southern areas were the main shipping channels connecting Wuxi and the Wangyu River, and the anthropogenic activities were relatively more intensive in the middle and southern area than in the northern area, which resulted in a higher trace metal pollution in sediments and greater ecological risk to benthic organisms.

5. CONCLUSION

The results show that Ni, Cu, Zn, and Cr, had higher contents in sediments than those of the geogenic background concentrations, indicating a significant impact of anthropogenic activities on the enrichment of trace pollutants in the given area.

According to the SOM cluster analysis and constrained PMF source apportionment, the primary human-related sources were agricultural, industrial and vehicular, and geogenic natural sources. Agricultural sources showed high contributions mainly in the middle area of the lake. Industrial and vehicular sources contributed significantly to the southern area of the lake. The geogenic natural sources had a relatively higher uncertainty than the other two sources, but the uncertainty can be acceptable. According to the results derived from the SCM and SERM, moderate and considerable contamination levels were mostly found in the lake, which was strongly related to human activities. Hg and Cd in the sediments had the potential to increase risk in the studied urban aquatic system.

ACKNOWLEDGEMENTS

The authors gratefully thank the colleagues from the Nanjing Institute of Geography and Limnology, Chinese Academy of Sciences for supporting this work. This work was jointly supported by the group to group exchange for academic talents (great!ipid4all) programme provided by the German Academic Exchange Service and the Graduate Academy of Technische Universität Dresden (PSP-Elements: F-003661-553-A2A-3410002/F-005268-536-900-2330000), State Major Science and Technology Program of Water Pollution Control and Treatment of China: Technology Development and Pilot Project on Reconstruction of Healthy Ecosystem in West Bank Lakes of Wangyu River (No. 2017ZX07204005), National Natural Science Foundation of China (No. 41877488), National Key Research and Development Program of China (No. 2018YFE0105900), and Construction Plan for Overseas Scientific Education Base of the Chinese Academy of Sciences (No. SAJC201609). The mention of trade names or commercial products does not constitute endorsement or recommendation for use. This manuscript has not been subjected to the required peer and policy review of the above agencies and, thus, does not reflect the views of the above agencies, nor should any official endorsement be inferred.

Table 1 Comparison between the trace metal (Cd, Mn, Ni, Cu, Zn, As, Cr, Hg, and Pb) concentrations in the study, the geogenic background, and the average concentrations in other rivers/lakes in China (mg/kg dry weight).

Study area		Cr	Mn	Ni	Cu	Zn	As	Cd	Hg	Pb
This study	Mean	153.00	697.00	89.00	104.00	418.00	14.00	0.10	0.17	17.40
	Median	129.00	645.00	87.00	90.00	375.00	13.85	0.09	0.17	17.10
	Range	75.00–533.00	340.00–1170.00	59.00–183.00	31.00–479.00	203.00–895.00	7.82–21.50	0.02–0.37	0.04–0.38	8.50–27.80
	CV (%)	60.10	33.66	28.67	78.12	42.47	30.72	62.58	44.65	29.89
	Background (mg/kg)[1]	83.000	/	35.200	27.000	69.000	9.200	0.082	0.060	23.900
Taihu Basin (Bian et al., 2016)		89.42	/	43.00	86.00	147.20	10.98	0.66	0.13	50.83
Yangtze-Taihu section (Qin et al., 2015)		65.79	/	/	26.60	124.73	10.57	1.78	/	44.11
Han River (Cao et al., 2018)		77.50	/	29.60	46.00	144.20	/	0.26	/	40.10
Chaohu Lake (Fang et al., 2019a)		72.5		/	26.0	137.8	10.4	0.44	0.114	47.1
East Lake, Wuhan (Jiang et al., 2018)		151.00	/	27.60	56.10	224.00	200.00	0.92	0.18	7.60
Lihu Lake (Wang et al., 2019a)		77.400	/	29.100	31.000	102.200	12.400	0.360	0.097	74.500
Poyang Lake (Dai et al., 2018)		135.9	/	/	62.0	132.9	/	0.7	/	77.4
Yellow River (Yan et al., 2016)		62.400	/	23.600	40.700	68.400	2.460	0.085	/	15.200

Weihe Basin (Wang et al., 2019b)	75.70	/	26.64	21.80	70.79	/	0.19	/	20.81

Note:

[1]The background values of trace elements were referenced from their content contained in Xiashu loess owing to the strong effect of loess on the river sediments in the Taihu Basin (Bian et al., 2016)

Figure captions

Fig. 1 a) Map of the study area of Wanshan Lake, Wuxi, China and b-e) spatial distribution of the trace metal (Cd, Mn, Ni, Cu, Zn, As, Cr, Hg, and Pb) contents in sediments.

Fig. 2 a) Component planes of trace metals obtained by performing self-organising map (SOM) analysis and b) the map unit labels with clusters I–IV derived from the K-means algorithm. The hexagon in a certain position corresponds to the same map unit.

Fig. 3 a) Fractional contributions of each factor to the trace metal content in sediments and spatial contribution distribution percentage of b) agricultural sources, c) industrial and vehicular sources, and d) geogenic natural sources among the total pollution contribution in Wanshan Lake without considering M6.

Fig. 4 Simulated concentrations Upper uncertainty intervals of the trace metals by BS method and DISP method for each factor.

Fig. 5 Rose chart of the a) contamination level and b) ecological risk of trace metals in sediments through the stochastic contamination model (SCM) and risk determination model (SERM). The angular axis presents the probability of a variable in a specific class.

Fig. 1

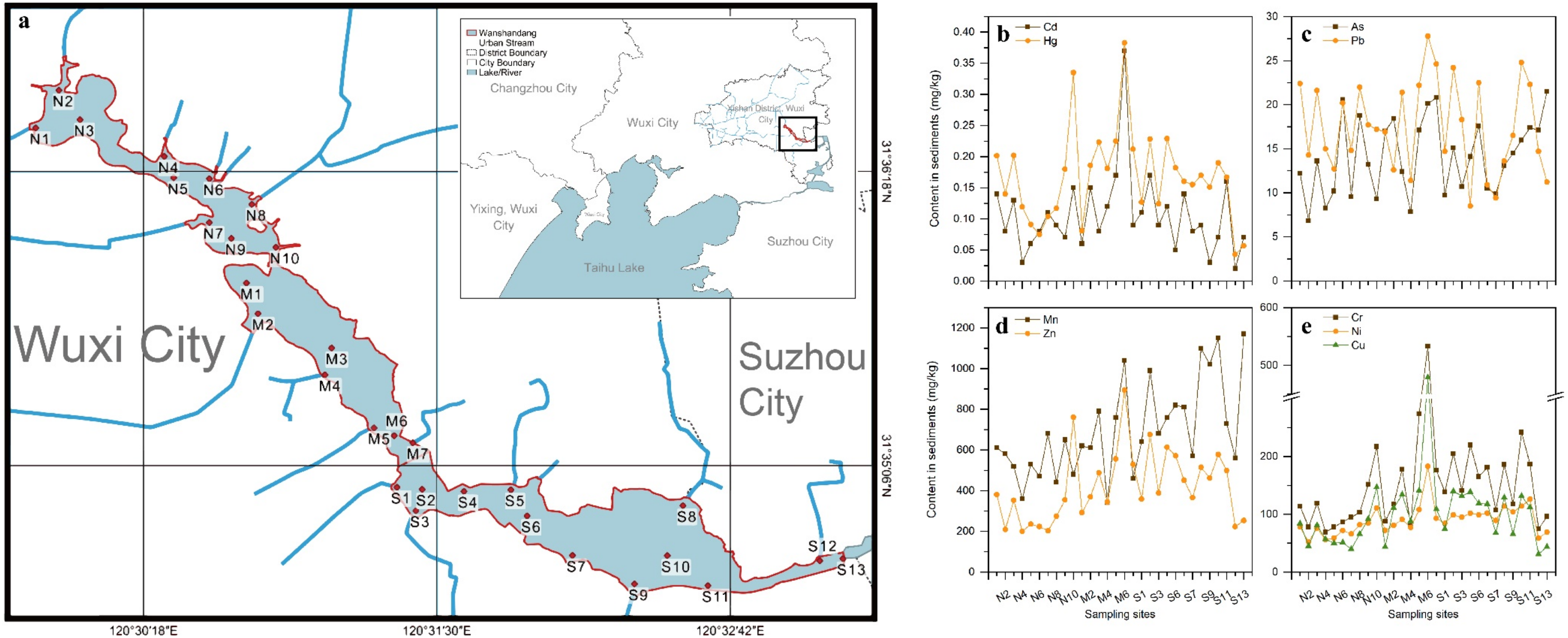
a
Wanshandang
Urban Stream
District Boundary
City Boundary
Lake/River
Changzhou City
Wuxi City
Xishan District, Wuxi City
Yixing, Wuxi City
Suzhou City
Taihu Lake
Wuxi City
Suzhou City
N1
N2
N3
N4
N5
N6
N7
N8
N9
N10
M1
M2
M3
M4
M5
M6
M7
S1
S2
S3
S4
S5
S6
S7
S8
S9
S10
S11
S12
S13
120°30'18"E
120°31'30"E
120°32'42"E
31°36'18"N
31°35'06"N
b
Cd
Hg
c
As
Pb
d
Mn
Zn
e
Cr
Ni
Cu
Content in sediments (mg/kg)
Sampling sites

Fig. 2

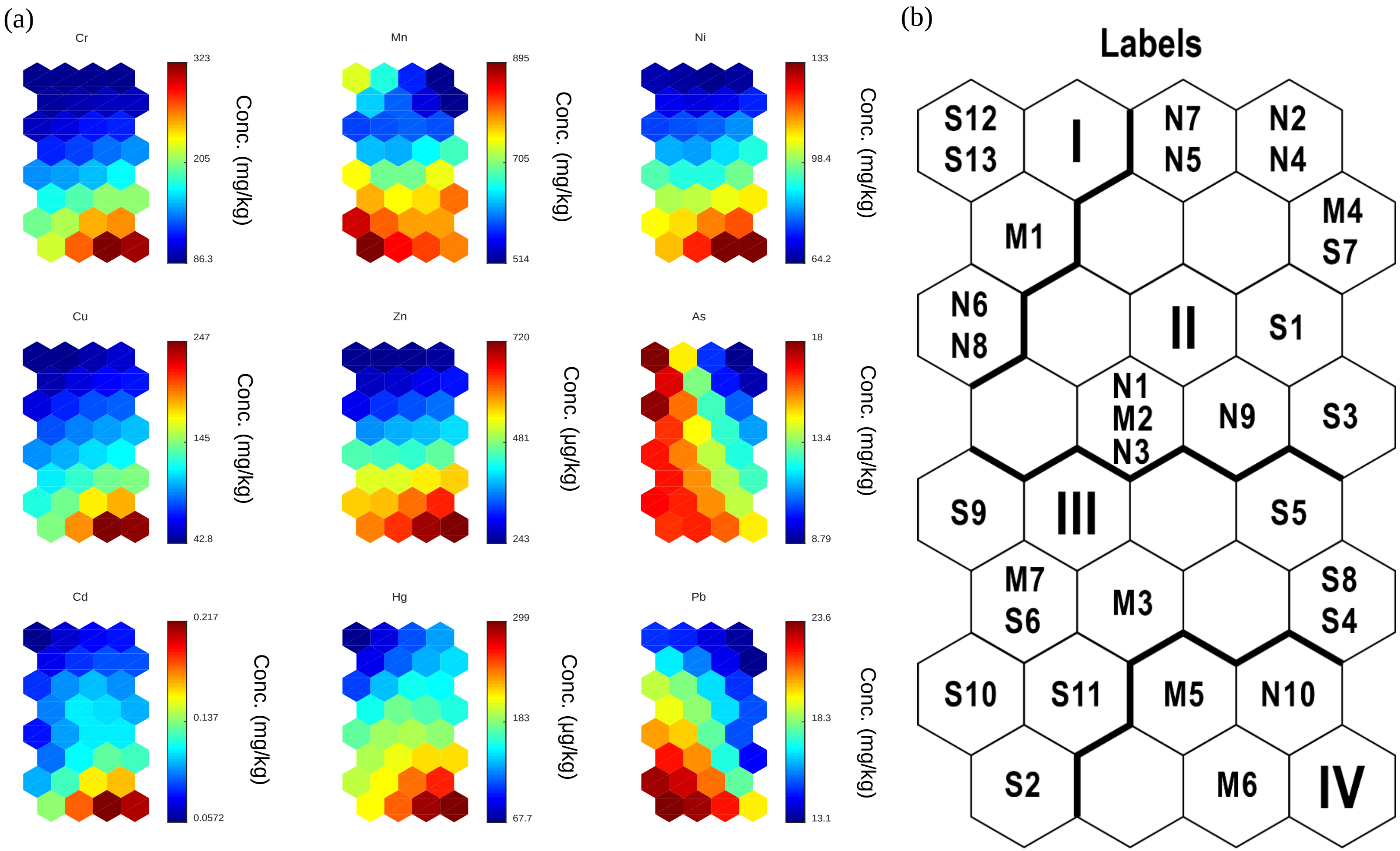

(a)
Cr
323
205
86.3
Conc. (mg/kg)
Mn
895
705
514
Conc. (mg/kg)
Ni
133
98.4
64.2
Conc. (mg/kg)
Cu
247
145
42.8
Conc. (mg/kg)
Zn
720
481
243
Conc. (µg/kg)
As
18
13.4
8.79
Conc. (mg/kg)
Cd
0.217
0.137
0.0572
Conc. (mg/kg)
Hg
299
183
67.7
Conc. (µg/kg)
Pb
23.6
18.3
13.1
Conc. (mg/kg)
(b)
Labels
S12 S13
I
N7 N5
N2 N4
M1
M4 S7
N6 N8
II
S1
N1 M2 N3
N9
S3
S9
III
S5
M7 S6
M3
S8 S4
S10
S11
M5
N10
S2
M6
IV

Fig. 3

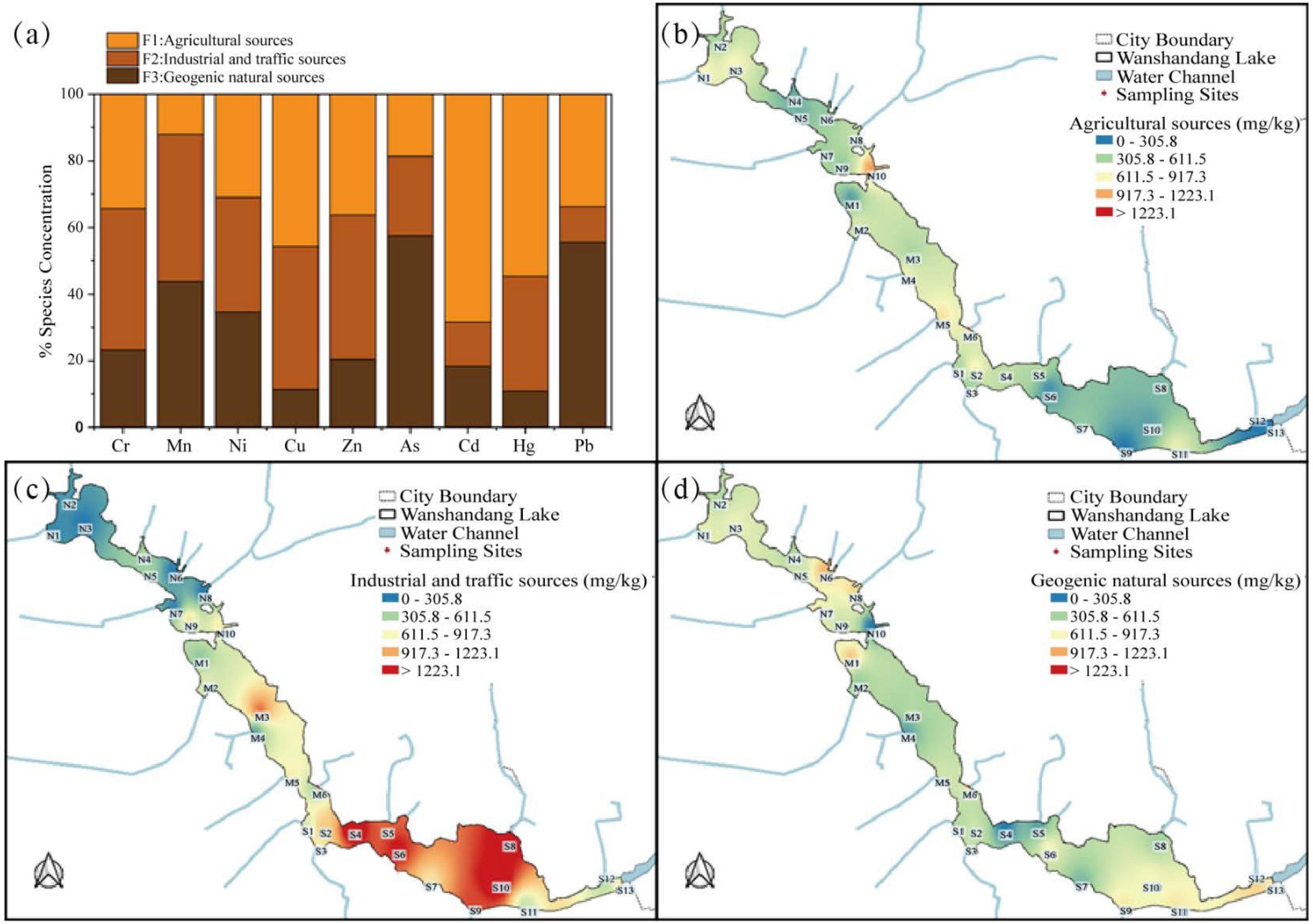

(a)
F1:Agricultural sources
F2:Industrial and traffic sources
F3:Geogenic natural sources
% Species Concentration
0
20
40
60
80
100
Cr
Mn
Ni
Cu
Zn
As
Cd
Hg
Pb
(b)
City Boundary
Wanshandang Lake
Water Channel
Sampling Sites
Agricultural sources (mg/kg)
0 - 305.8
305.8 - 611.5
611.5 - 917.3
917.3 - 1223.1
> 1223.1
(c)
City Boundary
Wanshandang Lake
Water Channel
Sampling Sites
Industrial and traffic sources (mg/kg)
0 - 305.8
305.8 - 611.5
611.5 - 917.3
917.3 - 1223.1
> 1223.1
(d)
City Boundary
Wanshandang Lake
Water Channel
Sampling Sites
Geogenic natural sources (mg/kg)
0 - 305.8
305.8 - 611.5
611.5 - 917.3
917.3 - 1223.1
> 1223.1

Fig. 4

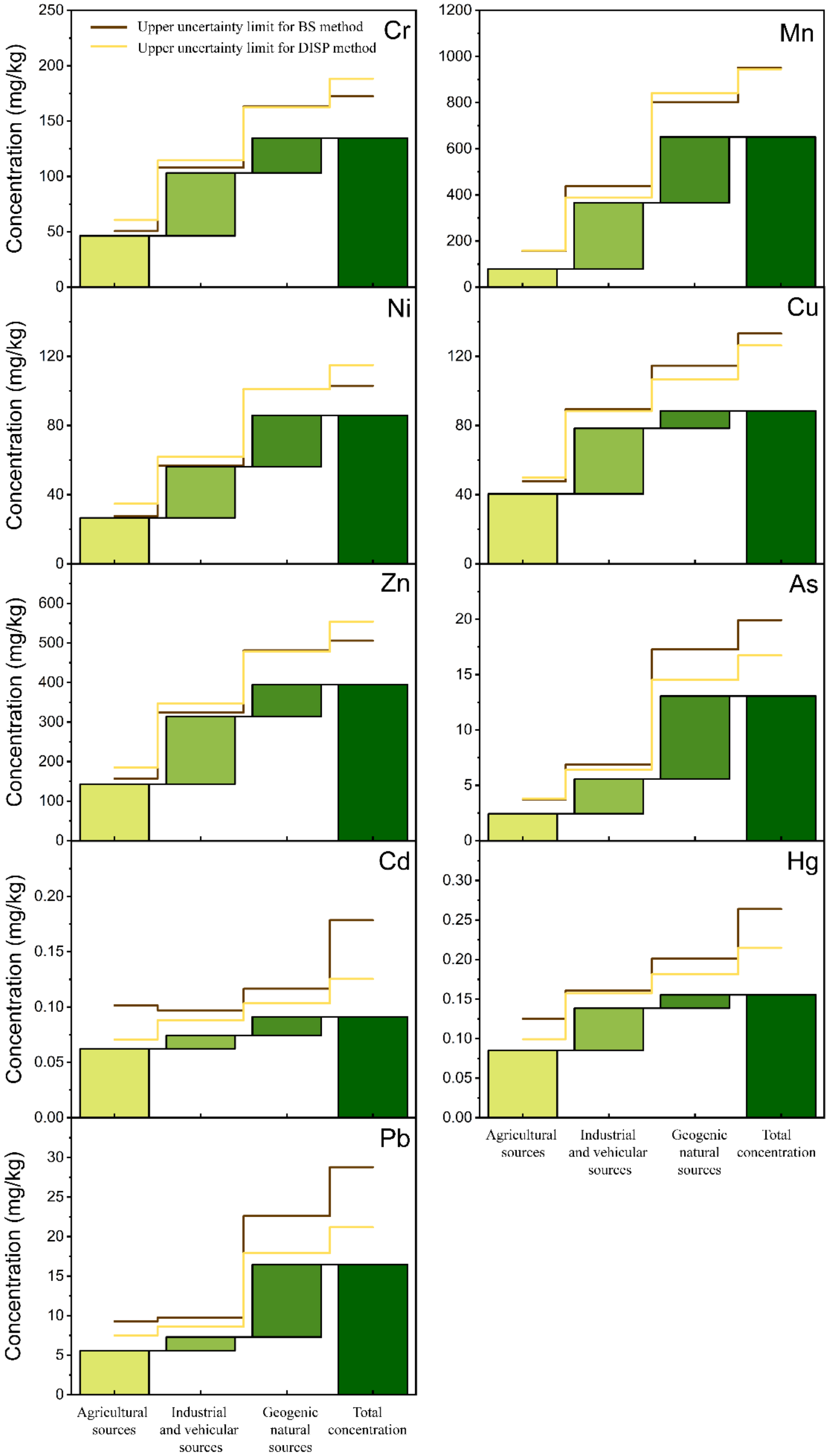

Upper uncertainty limit for BS method
Upper uncertainty limit for DISP method
Cr
Mn
Ni
Cu
Zn
As
Cd
Hg
Pb
Concentration (mg/kg)
Agricultural sources
Industrial and vehicular sources
Geogenic natural sources
Total concentration

Fig. 5

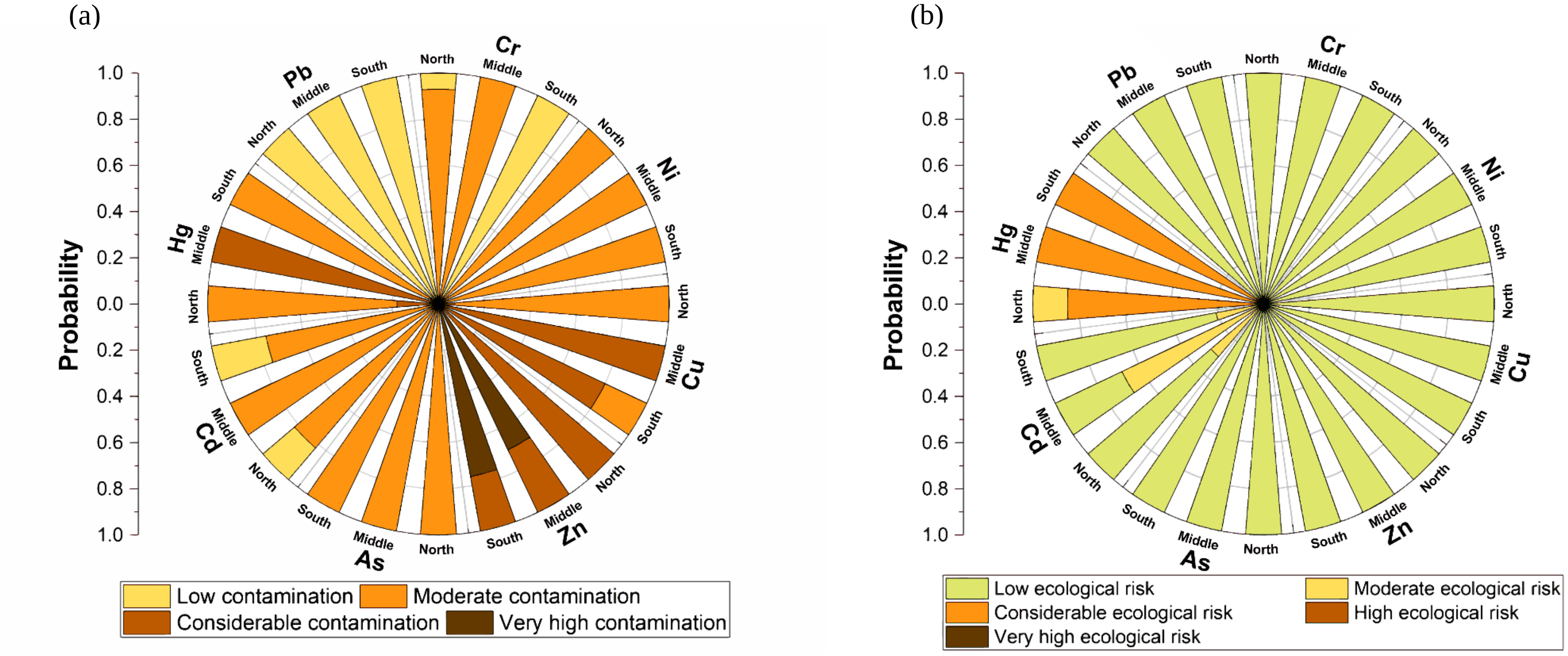
(a)
(b)
Probability
1.0
0.8
0.6
0.4
0.2
0.0
Cr
Ni
Cu
Zn
As
Cd
Hg
Pb
North
Middle
South
Low contamination
Moderate contamination
Considerable contamination
Very high contamination
Low ecological risk
Moderate ecological risk
Considerable ecological risk
High ecological risk
Very high ecological risk

Reference

Adekola, F., Eletta, O., 2007. A study of heavy metal pollution of Asa River, Ilorin. Nigeria; trace metal monitoring and geochemistry.

Alvarez-Guerra, M., González-Piñuela, C., Andrés, A., Galán, B., Viguri, J.R., 2008. Assessment of Self-Organizing Map artificial neural networks for the classification of sediment quality. Environment International 34, 782-790.

Ayeni, A.O., Balogun, I.I., Soneye, A.S.O., 2011. Seasonal Assessment of Physico—chemical Concentration of Polluted Urban River: A Case of Ala River in Southwestern—Nigeria. Research Journal of Environmental Sciences 5, 22-35.

Bian, B., Zhou, Y., Fang, B.B., 2016. Distribution of heavy metals and benthic macroinvertebrates: Impacts from typical inflow river sediments in the Taihu Basin, China. Ecological Indicators 69, 348-359.

Brown, S.G., Eberly, S., Paatero, P., Norris, G.A., 2015a. Methods for estimating uncertainty in PMF solutions: Examples with ambient air and water quality data and guidance on reporting PMF results. Science of the total environment 518-519, 626-635.

Brown, S.G., Eberly, S., Paatero, P., Norris, G.A., 2015b. Methods for estimating uncertainty in PMF solutions: Examples with ambient air and water quality data and guidance on reporting PMF results. Science of the total environment 518, 626-635.

Cabrera, F., Clemente, L., Barrientos, E.D., López, R., Murillo, J., 1999. Heavy metal pollution of soils affected by the Guadiamar toxic flood. Science of The Total Environment 242, 117-129.

Cao, Y., Lei, K., Zhang, X., Xu, L., Lin, C., Yang, Y., 2018. Contamination and ecological risks of toxic metals in the Hai River, China. Ecotoxicology and environmental safety 164, 210-218.

Chen, H., Teng, Y., Li, J., Wu, J., Wang, J., 2016. Source apportionment of trace metals in river sediments: A comparison of three methods. Environmental Pollution 211, 28-37.

Chen, J., Theller, L., Gitau, M.W., Engel, B.A., Harbor, J.M., 2017. Urbanization impacts on surface runoff of the contiguous United States. Journal of environmental management 187, 470-481.

Chen, L., Hu, B.X., Dai, H., Zhang, X., Xia, C.-A., Zhang, J., 2019. Characterizing microbial diversity and community composition of groundwater in a salt-freshwater transition zone. Science of the total environment 678, 574-584.

Chen, X., Liu, X., Liu, M., Yang, Y., Wu, S., Wang, C., 2018. Molecular characterization of PAHs based on land use analysis and multivariate source apportionment in multiple phases of the Yangtze estuary, China. Environmental Science: Processes & Impacts 20, 531-543.

Chetelat, B., Gaillardet, J., 2005. Boron isotopes in the Seine River, France: a probe of anthropogenic contamination. Environmental Science & Technology 39, 2486-2493.

Cheung, K., Poon, B., Lan, C., Wong, M.H., 2003. Assessment of metal and nutrient concentrations in river water and sediment collected from the cities in the Pearl River Delta, South China. Chemosphere 52, 1431-1440.

Comero, S., Capitani, L., Gawlik, B., 2009. Positive Matrix Factorisation (PMF). An introduction to the chemometric evaluation of environmental monitoring data using PMF. JRC Scientific and Technical reports EUR 23946 EN–2009. European Commission Joint Research Centre. Institute for Environment and Sustainability, Ispra, Italy, 1-59.

Dai, L., Wang, L., Li, L., Liang, T., Zhang, Y., Ma, C., Xing, B., 2018. Multivariate geostatistical analysis and source identification of heavy metals in the sediment of Poyang Lake in China. Science of The Total Environment 621, 1433-1444.

Davies, D.L., Bouldin, D.W., 1979. A cluster separation measure. IEEE transactions on pattern analysis and machine intelligence, 224-227.

Fang, T., Lu, W., Cui, K., Li, J., Yang, K., Zhao, X., Liang, Y., Li, H., 2019a. Distribution, bioaccumulation and trophic transfer of trace metals in the food web of Chaohu Lake, Anhui, China. Chemosphere 218, 1122-1130.

Fang, X., Peng, B., Wang, X., Song, Z., Zhou, D., Wang, Q., Qin, Z., Tan, C., 2019b. Distribution, contamination and source identification of heavy metals in bed sediments from the lower reaches of the Xiangjiang River in Hunan province, China. Science of The Total Environment 689, 557-570.

Feng, Y., Bao, Q., Xiao, X., Lin, M., 2019a. Geo-accumulation vector model for evaluating the heavy metal pollution in the sediments of Western Dongting Lake. Journal of Hydrology 573, 40-48.

Feng, Y., Chenglin, L., Bowen, W., 2019b. Evaluation of heavy metal pollution in the sediment of Poyang Lake based on stochastic geo-accumulation model (SGM). Science of The Total Environment 659, 1-6.

Fu, J., Hu, X., Tao, X., Yu, H., Zhang, X., 2013. Risk and toxicity assessments of heavy metals in sediments and fishes from the Yangtze River and Taihu Lake, China. Chemosphere 93, 1887-1895.

Gu, Y.-G., Gao, Y.-P., 2019. An unconstrained ordination- and GIS-based approach for identifying anthropogenic sources of heavy metal pollution in marine sediments. Marine Pollution Bulletin 146, 100-105.

Gugamsetty, B., Wei, H., Liu, C.-N., Awasthi, A., Hsu, S.-C., Tsai, C.-J., Roam, G.-D., Wu, Y.-C., Chen, C.-F., 2012. Source characterization and apportionment of PM10, PM2. 5 and PM0. 1 by using positive matrix factorization. Aerosol Air Qual. Res 12, 476-491.

Guo, C., Chen, Y., Xia, W., Qu, X., Yuan, H., Xie, S., Lin, L.-S., 2020. Eutrophication and heavy metal pollution patterns in the water suppling lakes of China's south-to-north water diversion project. Science of The Total Environment 711, 134543.

Hakanson, L., 1980. An ecological risk index for aquatic pollution control. A sedimentological approach. Water Research 14, 975-1001.

Hossain, M.B., Shanta, T.B., Ahmed, A.S.S., Hossain, M.K., Semme, S.A., 2019. Baseline study of heavy metal contamination in the Sangu River estuary, Chattogram, Bangladesh. Marine Pollution Bulletin 140, 255-261.

Jain, C., 2004. Metal fractionation study on bed sediments of River Yamuna, India. Water Research 38, 569-578.

Jain, S., Sharma, S.K., Mandal, T.K., Saxena, M., 2018. Source apportionment of PM10 in Delhi, India using PCA/APCS, UNMIX and PMF. Particuology 37, 107-118.

Ji, Z., Zhang, Y., Zhang, H., Huang, C., Pei, Y., 2019. Fraction spatial distributions and ecological risk assessment of heavy metals in the sediments of Baiyangdian Lake. Ecotoxicology and environmental safety 174, 417-428.

Jiang, Q., Liu, M., Wang, J., Liu, F., 2018. Feasibility of using visible and near-infrared reflectance spectroscopy to monitor heavy metal contaminants in urban lake sediment. CATENA 162, 72-79.

JPDWR, 2006. Lake protection plan Jiangsu Province. Jiangsu Province Department Of Water Resources, Jiangsu Province, China, p. 31.

Kaeseberg, T., Zhang, J., Schubert, S., Oertel, R., Siedel, H., Krebs, P., 2018. Sewer sediment-bound antibiotics as a potential environmental risk: Adsorption and desorption affinity of 14 antibiotics and one metabolite. Environmental pollution 239, 638-647.

Kalteh, A.M., Hjorth, P., Berndtsson, R., 2008. Review of the self-organizing map (SOM) approach in water resources: Analysis, modelling and application. Environmental modelling & software 23, 835-845.

Kiang, M.Y., 2001. Extending the Kohonen self-organizing map networks for clustering analysis. Computational Statistics & Data Analysis 38, 161-180.

Kohonen, T., 1990. The self-organizing map. Proceedings of the IEEE 78, 1464-1480.

Li, F., Huang, J., Zeng, G., Yuan, X., Li, X., Liang, J., Wang, X., Tang, X., Bai, B., 2013. Spatial risk assessment and sources identification of heavy metals in surface sediments from the Dongting Lake, Middle China. Journal of Geochemical Exploration 132, 75-83.

Li, J., Li, F., Liu, Q., Zhang, Y., 2014. Trace metal in surface water and groundwater and its transfer in a Yellow River alluvial fan: Evidence from isotopes and hydrochemistry. Science of The Total Environment 472, 979-988.

Li, L., Jiang, M., Liu, Y., Shen, X., 2019a. Heavy metals inter-annual variability and distribution in the Yangtze River estuary sediment, China. Marine Pollution Bulletin 141, 514-520.

Li, R., Hua, P., Cai, J., Wang, X., Zhu, Y., Huang, Z., Li, P., Wang, Z., Bai, Y., Hu, B.X., 2019b. A sixteen-year reduction in the concentrations of aquatic PAHs corresponding to source shifts in the Elbe River, Germany. Journal of Cleaner Production.

Li, T., Sun, G., Yang, C., Liang, K., Ma, S., Huang, L., 2018a. Using self-organizing map for coastal water quality classification: Towards a better understanding of patterns and processes. Science of The Total Environment 628-629, 1446-1459.

Li, Y., Mei, L., Zhou, S., Jia, Z., Wang, J., Li, B., Wang, C., Wu, S., 2018b. Analysis of historical sources of heavy metals in Lake Taihu based on the positive matrix factorization model. International journal of environmental research and public health 15, 1540.

Liang, P., Wu, S.-C., Zhang, J., Cao, Y., Yu, S., Wong, M.-H., 2016. The effects of mariculture on heavy metal distribution in sediments and cultured fish around the Pearl River Delta region, south China. Chemosphere 148, 171-177.

Lin, C., He, M., Liu, X., Guo, W., Liu, S., 2013. Contamination and ecological risk assessment of toxic trace elements in the Xi River, an urban river of Shenyang city, China. Environmental monitoring and assessment 185, 4321-4332.

Lin, Q., Liu, E., Zhang, E., Li, K., Shen, J., 2016. Spatial distribution, contamination and ecological risk assessment of heavy metals in surface sediments of Erhai Lake, a large eutrophic plateau lake in southwest China. CATENA 145, 193-203.

Luo, Z., Shao, Q., Zuo, Q., Cui, Y., 2020. Impact of land use and urbanization on river water quality and ecology in a dam dominated basin. Journal of Hydrology, 124655.

Manousakas, M., Papaefthymiou, H., Diapouli, E., Migliori, A., Karydas, A.G., Bogdanovic-Radovic, I., Eleftheriadis, K., 2017. Assessment of PM2.5 sources and their corresponding level of uncertainty in a coastal urban area using EPA PMF 5.0 enhanced diagnostics. Science of The Total Environment 574, 155-164.

Marrugo-Negrete, J., Pinedo-Hernández, J., Díez, S., 2017. Assessment of heavy metal pollution, spatial distribution and origin in agricultural soils along the Sinú River Basin, Colombia. Environmental Research 154, 380-388.

Men, C., Liu, R., Wang, Q., Guo, L., Miao, Y., Shen, Z., 2019. Uncertainty analysis in source apportionment of heavy metals in road dust based on positive matrix factorization model and geographic information system. Science of The Total Environment 652, 27-39.

Nguyen, B.T., Do, D.D., Nguyen, T.X., Nguyen, V.N., Phuc Nguyen, D.T., Nguyen, M.H., Thi Truong, H.T., Dong, H.P., Le, A.H., Bach, Q.-V., 2020. Seasonal, spatial variation, and pollution sources of heavy metals in the sediment of the Saigon River, Vietnam. Environmental Pollution 256, 113412.

Ning, D., Huang, Y., Pan, R., Wang, F., Wang, H., 2014. Effect of eco-remediation using planted floating bed system on nutrients and heavy metals in urban river water and sediment: A field study in China. Science of the Total Environment 485-486, 596-603.

Niu, Y., Jiang, X., Wang, K., Xia, J., Jiao, W., Niu, Y., Yu, H., 2019. Meta analysis of heavy metal pollution and sources in surface sediments of Lake Taihu, China. Science of the Total Environment, 134509.

Norris, G., Duvall, R., Brown, S., Bai, S., 2014. EPA Positive Matrix Factorization (PMF) 5.0 fundamentals and User Guide Prepared for the US Environmental Protection Agency Office of Research and Development, Washington, DC. Inc., Petaluma.

Omwene, P.I., Öncel, M.S., Çelen, M., Kobya, M., 2018. Heavy metal pollution and spatial distribution in surface sediments of Mustafakemalpaşa stream located in the world's largest borate basin (Turkey). Chemosphere.

Özmen, H., Külahçı, F., Çukurovalı, A., Doğru, M., 2004. Concentrations of heavy metal and radioactivity in surface water and sediment of Hazar Lake (Elazığ, Turkey). Chemosphere 55, 401-408.

Paatero, P., S., E., G., B.S., A., N.G., 2014. Methods for estimating uncertainty in factor analytic solutions. Atmospheric Measurement Techniques 7, 781-797.

Pandey, M., Pandey, A.K., Mishra, A., Tripathi, B., 2015. Application of chemometric analysis and self organizing map-artificial neural network as source receptor modeling for metal speciation in river sediment. Environmental pollution 204, 64-73.

Park, J., Lee, S., Lee, E., Noh, H., Seo, Y., Lim, H., Shin, H., Lee, I., Jung, H., Na, T., Kim, S.D., 2019. Probabilistic ecological risk assessment of heavy metals using the sensitivity of resident organisms in four Korean rivers. Ecotoxicology and environmental safety 183, 109483.

Pekey, H., Karakaş, D., Bakoglu, M., 2004. Source apportionment of trace metals in surface waters of a polluted stream using multivariate statistical analyses. Marine Pollution Bulletin 49, 809-818.

Pinsino, A., Matranga, V., Roccheri, M.C., 2012. Manganese: a new emerging contaminant in the environment, Environmental contamination. IntechOpen.

Qin, H.-P., Khu, S.-T., Yu, X.-Y., 2010. Spatial variations of storm runoff pollution and their correlation with land-use in a rapidly urbanizing catchment in China. Science of The Total Environment 408, 4613-4623.

Qin, Y., Cao, W., Ma, Y., Zhang, L., Liu, Z., Chang, X., 2015. Distribution and standardized analysis of heavy metal among surface water, suspended solids and surface sediments in the Yangtze-Taihu water diversion section. Environ Poll Control 37, 5-9.

Quevauviller, P., Lavigne, R., Cortez, L., 1989. Impact of industrial and mine drainage wastes on the heavy metal distribution in the drainage basin and estuary of the Sado River (Portugal). Environmental Pollution 59, 267-286.

Raghunath, R., Tripathi, R., Kumar, A.V., Sathe, A., Khandekar, R., Nambi, K., 1999. Assessment of Pb, Cd, Cu, and Zn exposures of 6-to 10-year-old children in Mumbai. Environmental Research 80, 215-221.

Ruiz-Fernández, A.C., Frignani, M., Hillaire-Marcel, C., Ghaleb, B., Arvizu, M., Raygoza-Viera, J., Páez-Osuna, F., 2009. Trace metals (Cd, Cu, Hg, and Pb) accumulation recorded in the intertidal mudflat sediments of three coastal lagoons in the Gulf of California, Mexico. Estuaries and Coasts 32, 551-564.

Sharifi, Z., Hossaini, S.M., Renella, G., 2016. Risk assessment for sediment and stream water polluted by heavy metals released by a municipal solid waste composting plant. Journal of Geochemical Exploration 169, 202-210.

Shil, S., Singh, U.K., 2019. Health risk assessment and spatial variations of dissolved heavy metals and metalloids in a tropical river basin system. Ecological Indicators 106, 105455.

Sofowote, U.M., McCarry, B.E., Marvin, C.H., 2008. Source apportionment of PAH in Hamilton Harbour suspended sediments: comparison of two factor analysis methods. Environmental science & technology 42, 6007-6014.

Sutherland, R., 2000. Bed sediment-associated trace metals in an urban stream, Oahu, Hawaii. Environmental geology 39, 611-627.

Tomlinson, D., Wilson, J., Harris, C., Jeffrey, D., 1980. Problems in the assessment of heavy-metal levels in estuaries and the formation of a pollution index. Helgoländer meeresuntersuchungen 33, 566.

Tong, S.T.Y., Chen, W., 2002. Modeling the relationship between land use and surface water quality. Journal of environmental management 66, 377-393.

Varol, M., 2011. Assessment of heavy metal contamination in sediments of the Tigris River (Turkey) using pollution indices and multivariate statistical techniques. Journal of Hazardous Materials 195, 355-364.

Vesanto, J., Himberg, J., Alhoniemi, E., Parhankangas, J., 1999. Self-organizing map in Matlab: the SOM Toolbox, Proceedings of the Matlab DSP conference, pp. 16-17.

Vesanto, J., Himberg, J., Alhoniemi, E., Parhankangas, J., 2000. SOM toolbox for Matlab 5. Helsinki University of Technology, Finland 109.

Wang, L., Dai, L., Li, L., Liang, T., 2018. Multivariable cokriging prediction and source analysis of potentially toxic elements (Cr, Cu, Cd, Pb, and Zn) in surface sediments from Dongting Lake, China. Ecological Indicators 94, 312-319.

Wang, S., Wang, W., Chen, J., Zhao, L., Zhang, B., Jiang, X., 2019a. Geochemical baseline establishment and pollution source determination of heavy metals in lake sediments: A case study in Lihu Lake, China. Science of The Total Environment 657, 978-986.

Wang, X., Su, P., Lin, Q., Song, J., Sun, H., Cheng, D., Wang, S., Peng, J., Fu, J., 2019b. Distribution, assessment and coupling relationship of heavy metals and macroinvertebrates in sediments of the Weihe River Basin. Sustainable Cities and Society 50, 101665.

Wang, Z., Hua, P., Li, R., Bai, Y., Fan, G., Wang, P., Hu, B.X., Zhang, J., Krebs, P., 2019c. Concentration decline in response to source shift of trace metals in Elbe River, Germany: A long-term trend analysis during 1998–2016. Environmental pollution 250, 511-519.

Wijesiri, B., Liu, A., Deilami, K., He, B., Hong, N., Yang, B., Zhao, X., Ayoko, G., Goonetilleke, A., 2019. Nutrients and metals interactions between water and sediment phases: An urban river case study.

Environmental Pollution 251, 354-362.

Wu, J., Li, J., Teng, Y., Chen, H., Wang, Y., 2019. A partition computing-based positive matrix factorization (PC-PMF) approach for the source apportionment of agricultural soil heavy metal contents and associated health risks. Journal of Hazardous Materials, 121766.

Yan, N., Liu, W., Xie, H., Gao, L., Han, Y., Wang, M., Li, H., 2016. Distribution and assessment of heavy metals in the surface sediment of Yellow River, China. Journal of Environmental Sciences 39, 45-51.

Yang, J., Chen, L., Liu, L.-Z., Shi, W.-L., Meng, X.-Z., 2014. Comprehensive risk assessment of heavy metals in lake sediment from public parks in Shanghai. Ecotoxicology and environmental safety 102, 129-135.

Yang, Z., Wang, Y., Shen, Z., Niu, J., Tang, Z., 2009. Distribution and speciation of heavy metals in sediments from the mainstream, tributaries, and lakes of the Yangtze River catchment of Wuhan, China. Journal of Hazardous Materials 166, 1186-1194.

Yi, Y., Yang, Z., Zhang, S., 2011. Ecological risk assessment of heavy metals in sediment and human health risk assessment of heavy metals in fishes in the middle and lower reaches of the Yangtze River basin. Environmental Pollution 159, 2575-2585.

Yin, H., Gao, Y., Fan, C., 2011. Distribution, sources and ecological risk assessment of heavy metals in surface sediments from Lake Taihu, China. Environmental Research Letters 6, 044012.

Zaharescu, D.G., Hooda, P.S., Soler, A.P., Fernandez, J., Burghelea, C.I., 2009. Trace metals and their source in the catchment of the high altitude Lake Respomuso, Central Pyrenees. Science of The Total Environment 407, 3546-3553.

Zhang, G., Bai, J., Xiao, R., Zhao, Q., Jia, J., Cui, B., Liu, X., 2017a. Heavy metal fractions and ecological risk assessment in sediments from urban, rural and reclamation-affected rivers of the Pearl River Estuary, China. Chemosphere 184, 278-288.

Zhang, J., Hua, P., Krebs, P., 2015a. The build-up dynamic and chemical fractionation of Cu, Zn and Cd in road-deposited sediment. Science of the total environment 532, 723-732.

Zhang, J., Hua, P., Krebs, P., 2015b. The chemical fractionation and potential source identification of Cu, Zn and Cd on urban watershed. Water Science and Technology 72, 1428-1436.

Zhang, J., Hua, P., Krebs, P., 2017b. Influences of land use and antecedent dry-weather period on pollution level and ecological risk of heavy metals in road-deposited sediment. Environmental pollution 228, 158-168.

Zhang, J., Li, R., Zhang, X., Ding, C., Hua, P., 2019a. Traffic contribution to polycyclic aromatic hydrocarbons in road dust: A source apportionment analysis under different antecedent dry-weather periods. Science of the total environment 658, 996-1005.

Zhang, J., Wang, X., Zhu, Y., Huang, Z., Yu, Z., Bai, Y., Fan, G., Wang, P., Chen, H., Su, Y., Trujillo-González, J.M., Hu, B.X., Krebs, P., Hua, P., 2019b. The influence of heavy metals in road dust on the surface runoff quality: Kinetic, isotherm, and sequential extraction investigations. Ecotoxicology and Environmental Safety 176, 270-278.

Zhang, Y., Qu, W., 2001. Determination of heavy metals in the sediments from Taihu Lake and its environmental significance. Rock and Mineral Analysis 20, 34-36.

Zhang, Y., Su, Y., Liu, Z., Sun, K., Kong, L., Yu, J., Jin, M., 2018. Sedimentary lipid biomarker record of human-induced environmental change during the past century in Lake Changdang, Lake Taihu basin, Eastern China. Science of The Total Environment 613, 907-918.